

Light induced Josephson like current between two coupled nonlinear cavities coupled with a symmetrically positioned photonic crystal waveguide

To cite this article: Evgeny Bulgakov *et al* 2011 *J. Phys.: Condens. Matter* **23** 065304

View the [article online](#) for updates and enhancements.

Related content

- [Switching through symmetry breaking for transmission in a T-shaped photonic waveguide coupled with two identical nonlinear micro-cavities](#)
Evgeny Bulgakov and Almas Sadreev
- [Channel dropping via bound states in the continuum in a system of two nonlinear cavities between two linear waveguides](#)
Evgeny Bulgakov, Konstantin Pichugin and Almas Sadreev
- [Resonant excitation of off-channel localized impurity modes by a photonic crystal waveguide](#)
A R McGurn

Recent citations

- [Nonlinear Bound States in the Continuum in One-Dimensional Photonic Crystal Slab](#)
S.D. Krasikov *et al*
- [Frequency comb generation for wave transmission through the nonlinear dimer](#)
K N Pichugin and A F Sadreev
- [Channel dropping via bound states in the continuum in a system of two nonlinear cavities between two linear waveguides](#)
Evgeny Bulgakov *et al*



IOP | ebooks™

Bringing together innovative digital publishing with leading authors from the global scientific community.

Start exploring the collection—download the first chapter of every title for free.

Light induced Josephson like current between two coupled nonlinear cavities coupled with a symmetrically positioned photonic crystal waveguide

Evgeny Bulgakov^{1,2}, Konstantin Pichugin¹ and Almas Sadreev¹

¹ Kirensky Institute of Physics, 660036, Krasnoyarsk, Russia

² Siberian State Aerospace University, Krasnoyarsk Rabochii, 31, Krasnoyarsk, Russia

E-mail: almas@tnp.krasn.ru

Received 13 December 2010, in final form 7 January 2011

Published 27 January 2011

Online at stacks.iop.org/JPhysCM/23/065304

Abstract

We consider light transmission in a photonic crystal waveguide coupled with two identical nonlinear cavities positioned symmetrically beside the waveguide and coupled with each other. Using Green function theory we show three scenarios for the transmission. The first one inherits the linear case in which the light transmission preserves the symmetry. In the second scenario the symmetry is broken by the light intensities at the cavities. In the third scenario the intensities are equal but the phases of the complex amplitudes are different at the cavities. This results in a Josephson like current between the cavities. The model consideration agrees well with computations of the Poynting current in a photonic crystal waveguide coupled with two optical cavities filled with a Kerr material.

(Some figures in this article are in colour only in the electronic version)

1. Introduction

Symmetry breaking is at the heart of many physical phenomena. The spontaneous symmetry breaking for decrease of temperature in condensed matter physics is the most famous example [1]. In recent decades the phenomenon of symmetry breaking has been developed in nonlinear optics [2–5] with the establishment of one or more asymmetric states which no longer preserve the symmetry properties of the original solution. Recently Maes *et al* described symmetry breaking in a system with two coupled in-channel and off-channel nonlinear cavities (Fano resonators) aligned along a waveguide [6–8] that forms a Fabry–Pérot resonator. When equal power is injected on both sides of the waveguide, the system becomes symmetrical. Nevertheless the reflected output power might be different on the two sides of the cavities due to nonlinear effects. Symmetry breaking has been considered also for the case of many coupled nonlinear optical cavities [9, 10].

Here we consider two coupled identical cavities with a Kerr-based nonlinearity positioned beside and symmetrical

relative to the photonic waveguide (see figure 1(a)). Then the system does not require injection of equal power from both sides of the waveguide to be symmetrical. In the linear case both cavities are excited by a input wave with the same strength. In the nonlinear case this excitation shifts the resonance frequencies of the cavities. Due to the lack of the superposition principle for these two cavities, it is possible that the symmetric solution is no longer the only one at a certain input power or frequency of input light. Then the system can drift to a situation where one cavity is more excited than the other, and thus an asymmetric state arises. This scenario of symmetry breaking is well known [2, 3, 6, 7]. However we demonstrate a more subtle mechanism of symmetry breaking. The light is equal in intensity in the cavities but differs in phase. Then, similar to the Josephson current, a power current between the cavities arises if they are coupled.

2. Tight-binding model

We use the Green function approach developed in [11–15] for a 2D photonic crystal (PC) of dielectric rods with the dielectric

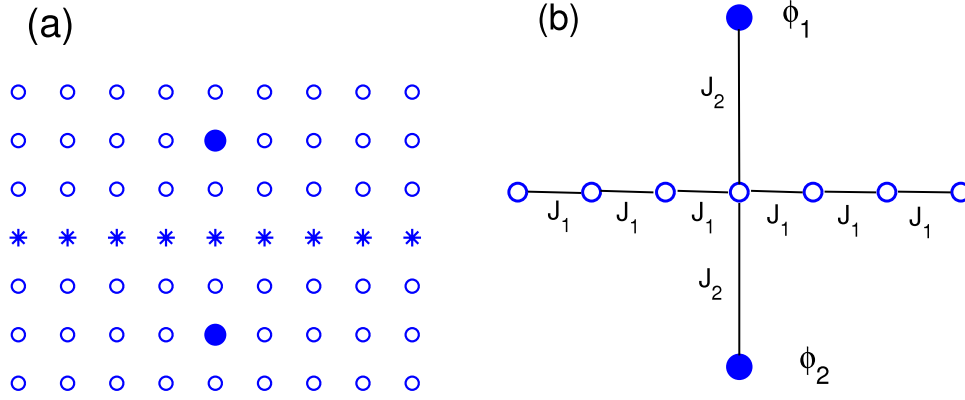


Figure 1. (a) Two cavity rods made from a Kerr medium marked by filled circles are inserted into the square lattice photonic crystal of dielectric rods with the dielectric constant ϵ_0 . The 1D waveguide is formed by substitution of a linear chain of rods by the rods with dielectric constant $\epsilon_w + \epsilon_0$ marked by stars. (b) The tight-binding version of the system: J_2 couples the chain and the cavities and J_4 couples the cavities to each other (not shown).

constant ϵ_0 . The PC holds the 1D cavity (waveguide) and two 0D cavities (nonlinear cavity rods) as shown in figure 1(a). Then the dielectric constant of the full system $\epsilon(\mathbf{x})$ is a sum of periodic perfect PC and cavity induced terms $\epsilon(\mathbf{x}) = \epsilon_{PC}(\mathbf{x}) + \delta\epsilon(\mathbf{x}|\mathbf{E})$, where $\delta\epsilon(\mathbf{x}|\mathbf{E}) = \epsilon_w(\mathbf{x}) + \epsilon_d(\mathbf{x}|\mathbf{E})$ is contributed by the waveguide and the two nonlinear cavities:

$$\epsilon_d(\mathbf{x}|\mathbf{E}) = [\epsilon_d - \epsilon_0 + \chi^{(3)}|\mathbf{E}(\mathbf{x})|^2] \sum_{j=1,2} \theta(\mathbf{x} - \mathbf{x}_j), \quad (1)$$

$$\epsilon_w(\mathbf{x}) = \epsilon_w \sum_{n=-\infty}^{\infty} \theta(\mathbf{x} - \mathbf{x}_n). \quad (2)$$

Here $\theta = 1$ inside the cavity rod and $\theta = 0$ outside, the nonlinear susceptibility $\chi^{(3)}$ is due to the Kerr effect. Then the TM electric field directed along the rods of the PC, $\mathbf{E}(\mathbf{x}, t) = \mathbf{E}(\mathbf{x})e^{i\omega t}$, satisfies the integral equation

$$\mathbf{E}(\mathbf{x}) = \frac{\omega^2}{c^2} \int d^2\mathbf{y} \mathbf{G}(\mathbf{x}, \mathbf{y}|\omega) \delta\epsilon(\mathbf{y}|\mathbf{E}) \mathbf{E}(\mathbf{y}), \quad (3)$$

where $\mathbf{G}(\mathbf{x}, \mathbf{y}|\omega)$ is the Green function of the ideal 2D PC of the rods which was calculated in [11] for the square lattice PC. If the radius of the cavity rods is sufficiently small in comparison to the wavelength of the EM wave, we can write equation (3) as the discrete nonlinear equation [11–13]

$$\mathbf{E}_n = \sum_m \mathbf{J}_{n-m}(\omega) \delta\epsilon_m \mathbf{E}_m, \quad (4)$$

where $\mathbf{J}_{n-m}(\omega) = \sigma \frac{\omega^2}{c^2} \mathbf{G}(\mathbf{x}_n, \mathbf{x}_m|\omega)$, σ is the cross-section of the rods, and \mathbf{n}, \mathbf{m} run over sites of the centers of the cavities (marked by stars and filled circles in figure 1(a)).

We use the nearest-neighbor approximation and write (4) as a tight-binding linear chain coupled with two nonlinear cavities:

$$\left[\frac{1}{\epsilon_w} - \mathbf{J}_0(\omega) \right] \mathbf{E}_n = \mathbf{J}_1(\mathbf{E}_{n+1} + \mathbf{E}_{n-1}) + \delta_{n,0} \frac{\mathbf{J}_2}{\epsilon_w} (\delta\epsilon_1 \phi_1 + \delta\epsilon_2 \phi_2), \quad (5)$$

$$[1 - \delta\epsilon_1 \mathbf{J}_0(\omega)] \phi_1 = \mathbf{J}_2 \epsilon_w \mathbf{E}_0 + \mathbf{J}_4 \delta\epsilon_2 \phi_2,$$

$$[1 - \delta\epsilon_2 \mathbf{J}_0(\omega)] \phi_2 = \mathbf{J}_2 \epsilon_w \mathbf{E}_0 + \mathbf{J}_4 \delta\epsilon_1 \phi_1,$$

where $\delta\epsilon_j = \epsilon_d - \epsilon_0 + \chi^{(3)}|\phi_j|^2$, $j = 1, 2$. The model is shown in figure 1(b) and consists of a linear infinitely long tight-binding chain represented by amplitudes \mathbf{E}_n whose spectrum is given by the dispersion equation $\mathbf{J}_0(\omega) = \frac{1}{\epsilon_w} - 2\mathbf{J}_1 \cos k$, and two nonlinear cavities represented by amplitudes ϕ_1, ϕ_2 . The coupling \mathbf{J}_2 connects the cavities and the chain and the coupling \mathbf{J}_4 connects the cavities.

We introduce here for computations the couplings \mathbf{J}_m computed in [13] for the simple square lattice (lattice constant $a = 0.5 \mu\text{m}$) of cylindrical rods of radius $0.18a$ with dielectric constant $\epsilon_0 = 11.56$ (GaAs at the wavelength $1.5 \mu\text{m}$) in air. For simplicity we ignore the frequency dependence in all couplings: $\mathbf{J}_1 = 0.04$, $\mathbf{J}_2 = -0.01$, $\mathbf{J}_4 = -0.001$, except $\mathbf{J}_0(\omega) = 1.11(\omega - 0.47)$ where the frequency here and in what follows is given in terms of $\frac{2\pi c}{a}$. The electric field is taken in terms of $\mathbf{E}_0 = 0.16 (\text{erg cm}^{-3})^{1/2}$ that corresponds to the typical incident power per length 100 mW/a . Furthermore we take the nonlinear refractive index $n_2 = 2.4 \times 10^{-12} \text{ cm}^2 \text{ W}^{-1}$. Then we obtain that the dimensionless Kerr coefficient of nonlinearity $\lambda = \chi^{(3)} \mathbf{E}_0^2 = 0.05$. These dimensionless parameters are used in all our numerical calculations.

Removing a row of rods creates the 1D PC waveguide which supports a single band of a guided monopole mode for TM polarization spanning from 0.315 to the upper band edge 0.41 [16], $\epsilon_w = 1 - \epsilon_0 = -10.56$. We substitute two rods by nonlinear ones with dielectric constant $\epsilon_d = 3$ as given by equation (1) and shown in figure 1(a). The tight-binding model (5) is close to that used in [13, 14] and holds the nonlinear terms not only in the equations for the cavity amplitudes ϕ_j , $j = 1, 2$ but in the couplings between the linear chain and the nonlinear cavities too.

For the chain we write the solution as $\mathbf{E}_n = \mathbf{E}_{in} e^{ikn} + r e^{-ikn}$, if $n \leq 0$, and $\mathbf{E}_n = t e^{ikn}$, if $n \geq 0$. Here \mathbf{E}_{in} is the amplitude of the incident wave, $|r|^2/\mathbf{E}_{in}^2$ and $|t|^2/\mathbf{E}_{in}^2$ are the reflection and transmission, respectively. Substituting this solution into equation (5) one can obtain the following equations for the cavity's amplitudes only:

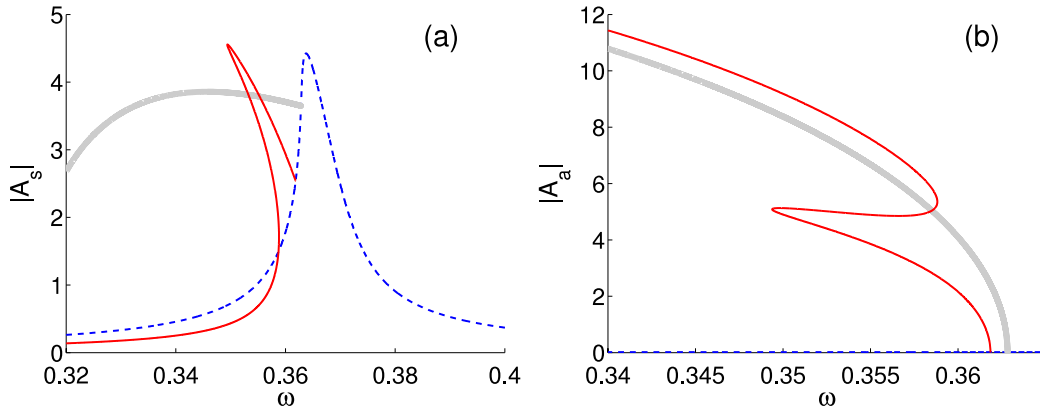


Figure 2. The frequency behavior of the even $A_s = \phi_1 + \phi_2$ (a) and odd $A_a = \phi_1 - \phi_2$ (b) mode amplitudes for $E_{in} = 0.5$, $\lambda = 0.05$ and the parameters of the tight-binding model (5) given in section 2. Here and in all forthcoming figures the dashed blue line shows the symmetrical branch with $A_a = 0$. The solid red line shows the symmetry breaking branch with $l_1 \neq l_2$. The gray thick solid line shows the phase parity breaking branch.

$$[1 - H_{eff}(\omega)] \begin{pmatrix} \phi_1 \\ \phi_2 \end{pmatrix} = J_2 \epsilon_w E_{in} \begin{pmatrix} 1 \\ 1 \end{pmatrix}, \quad (6)$$

$$H_{eff} = \begin{pmatrix} (J_0(\omega) + i\Gamma_k)\delta\epsilon_1 & (J_4 + i\Gamma_k)\delta\epsilon_2 \\ (J_4 + i\Gamma_k)\delta\epsilon_1 & (J_0(\omega) + i\Gamma_k)\delta\epsilon_2 \end{pmatrix},$$

where $\Gamma_k = \frac{J_2^2}{2J_1 |\sin k|}$. Equation (6) is a particular case of the Lippmann–Schwinger equation [17, 18] and is close to the coupled mode theory of two nonlinear cavities derived in [19], however with an important difference. The difference is that a nonlinear term is input not only into the diagonal matrix elements of H_{eff} but also into the non-diagonal matrix elements.

3. Symmetry preserving branch

The amplitudes ϕ_j of the nonlinear cavities are given by the inverse of the matrix $1 - H_{eff}(\omega)$ whose matrix elements, in turn, depend on the intensities $l_j = |\phi_j|^2$. That results in two equations of self-consistency which can be written analytically similarly to those given in [17, 19]. However in the present Green function approach the equations are too cumbersome. We present here the numerical results only.

The first solution is $l = l_1 = l_2$ which preserves the symmetry so that

$$\phi_1 = \phi_2 = \frac{J_2 \epsilon_w E_{in}}{1 - (J_0(\omega) + J_4 + 2i\Gamma_k)\delta\epsilon}, \quad (7)$$

as follows from (6), where $\delta\epsilon = \epsilon_d - \epsilon_0 + \lambda l$. The incident wave excites only the symmetric even mode $A_s = \phi_1 + \phi_2$ with the resonance frequency defined by the equation $\delta\epsilon(l)[J_0(\omega) + J_4] = 1$ and with the doubled width $2\Gamma_k$. With growth of the amplitude of the incident wave E_{in} the resonance frequency shifts to give rise to a bistability. The second odd mode $A_a = \phi_1 - \phi_2$ is not supported by the incident wave as shown in figure 2(b) by the dashed line. That mode is uncoupled from the leads and therefore is the bound state in continuum (BSC) with discrete frequency defined by the equation

$$(\epsilon_d - \epsilon_0)(J_0(\omega_c) - J_4) = 1. \quad (8)$$

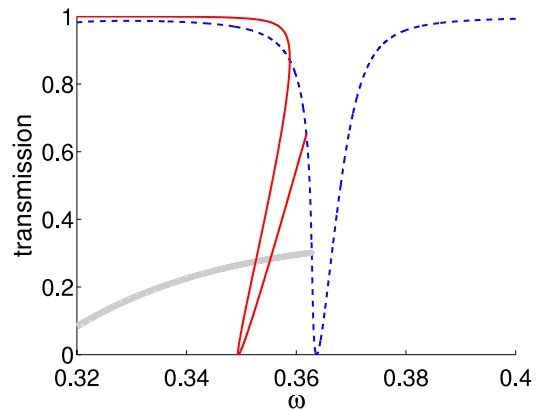


Figure 3. The transmission as a function of frequency for $E_{in} = 0.5$.

It is the simplest symmetry mechanism which gives rise to the BSC, as was presented in [19, 20].

The self-consistency equation for the symmetry preserving branch $l = l_1 = l_2$ is enormously simplified:

$$l([1 - (J_0(\omega) + J_4)\delta\epsilon]^2 + 4\Gamma_k^2 \delta\epsilon^2) = (J_2 \epsilon_w E_{in})^2. \quad (9)$$

It is very similar to the equation of self-consistency for a single off-channel nonlinear cavity [17, 21]. The transmission amplitude is given by the equation [17]

$$t = E_{in} + r = E_{in} + \frac{i\Gamma_k}{\epsilon_w J_2} \sum_j \delta\epsilon_j \phi_j. \quad (10)$$

The transmission for the symmetry preserving branch is shown in figure 3 by the dashed line.

4. The symmetry breaking branch

If the cavities were linear the symmetry preserving branch would be the only one that would follow from symmetry arguments based on the linear transformations. However in the nonlinear case these arguments are not true. The numerical solution, indeed, reveals two equivalent branches, the first

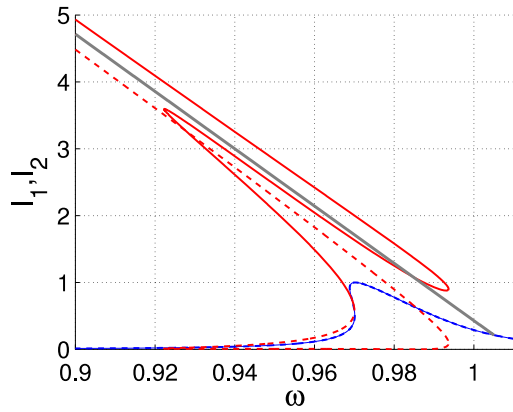


Figure 4. The intensities at the cavities as a function of the frequency of input wave for $E_{in} = 0.01$. The parameters of the tight-binding model (5) are collected in section 2. The intensities are shown by a dash-point blue line for the symmetry preserving branch and a thick gray line for the phase parity breaking branch. For the symmetry breaking branch the intensities I_1 and I_2 are different and shown by solid and dashed red lines.

with $I_1 > I_2$ and the second branch $\phi_1 \leftrightarrow \phi_2$, i.e., the nonlinearity gives rise to symmetry breaking below (above) a critical frequency for $\chi^{(3)} > 0$ ($\chi^{(3)} < 0$). We present here the solutions for the cavity's intensities as a function of the frequency and amplitude of the input wave as shown in figures 4 and 5.

However the frequency behavior of the even and odd mode amplitudes $|A_s|$ and $|A_a|$ shown in figure 2 is more comprehensible. The even mode A_s displays a resonance peak with the resonance width substantially less than the resonance width of the peak for the symmetry preserving branch (dashed line).

Correspondingly, the transmission in figure 3 demonstrates a narrow dip for the symmetry breaking branch. The degree of bistability mainly depends on the ratio between the input power proportional to E_{in}^2 and the resonance width [22]. Therefore, one can see that the bistability of the symmetry breaking branch is substantially more pronounced in comparison to the symmetry preserving branch. The resonance peak in $|A_s|$ for the symmetry breaking branch terminates at the frequency where the odd mode amplitude $|A_a|$ arises, as seen from figure 2(b). Close to this frequency the amplitude A_a has a

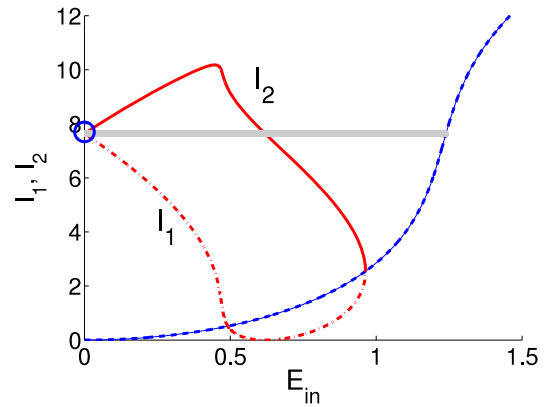


Figure 5. The intensities at the cavities as a function of E_{in} for $\omega = 0.36$. The point of the BSC is shown by a bold circle.

behavior typical of an order parameter in a phase transition of the second order. The dependence of A_a on the amplitude of the incident wave demonstrates the same behavior (see figure 6(b)).

5. The phase parity breaking branch

Finally, there is a unique branch which has equal intensities at the cavities but nevertheless the symmetry is broken by the phases of complex amplitudes ϕ_1 and ϕ_2 . This branch refers to the special case of equation (6) when the determinant of the matrix $1 - H_{eff}(\omega)$ equals zero, i.e., the inverse of the matrix does not exist. It occurs at

$$1 - J_0(\omega)(\delta\epsilon_1 + \delta\epsilon_2) + (J_0^2(\omega) - J_4^2)\delta\epsilon_1\delta\epsilon_2 = 0, \quad (11)$$

$$\delta\epsilon_1 + \delta\epsilon_2 = 2(J_0(\omega) - J_4)\delta\epsilon_1\delta\epsilon_2.$$

Simple algebra shows that equation (11) has the single solution

$$\delta\epsilon_1 = \delta\epsilon_2 = \delta\epsilon = \frac{1}{J_0(\omega) - J_4}, \quad (12)$$

with $\delta\epsilon_j = \epsilon_d - \epsilon_0 + \chi^{(3)}|\phi_j|^2$, $j = 1, 2$, i.e., the intensities at the cavities coincide. Although the inverse of the matrix $1 - H_{eff}(\omega)$ does not exist from equation (6) we obtain the particular solution

$$A_s = \phi_1 + \phi_2 = -J_2\epsilon_w E_{in} \frac{J_0(\omega) - J_4}{J_4 + i\Gamma_k}. \quad (13)$$

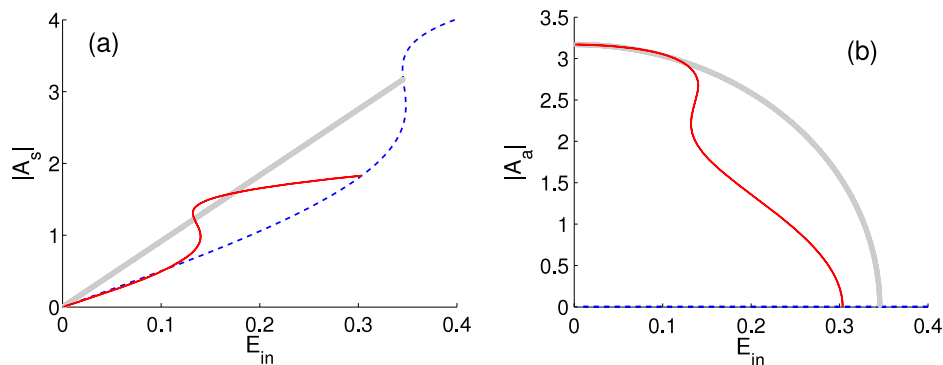


Figure 6. The amplitudes $|A_s|$ (a) and $|A_a|$ (b) as a function of the incident wave amplitude E_{in} .

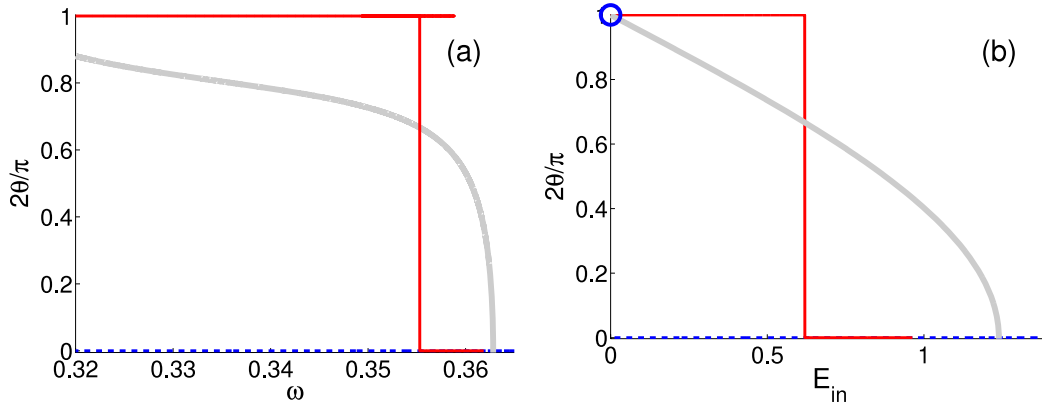


Figure 7. The difference between the phases of the cavity amplitudes ϕ_1 and ϕ_2 dependent on the frequency for fixed incident amplitude $E_{in} = 0.5$ (a) and on E_{in} for fixed frequency $\omega = 0.36$ (b). The BSC point is shown by the bold circle.

The moduli $|\phi_1| = |\phi_2|$ are fixed by equation (12) while the amplitudes are complex vectors as follows from equation (13): $\phi_1 = \sqrt{\Gamma} \exp(i(\alpha + \theta))$, $\phi_2 = \sqrt{\Gamma} \exp(i(\alpha - \theta))$. Then we obtain

$$4 \cos^2 \theta = \frac{J_2^2 E_{in}^2 \epsilon_W^2 \lambda (J_0(\omega) - J_4)^3}{(J_4^2 + \Gamma_k^2)(1 - (J_0(\omega) - J_4)(\epsilon_d - \epsilon_0))}, \quad (14)$$

$$\tan \alpha = -\Gamma_k / J_4. \quad (15)$$

Therefore, for this branch the EM oscillations in the cavities have the same intensity but different phases. The dependence of the phase difference on the frequency and the incident amplitude E_{in} is shown in figure 7. We emphasize that the phase difference 2θ has nontrivial behavior if the cavities are nonlinear ($\chi^{(3)} \neq 0$) and the incident wave is applied ($E_{in} \neq 0$) as follows from equation (14). For the symmetry preserving branch $\theta = 0$ (dashed line in figure 7), for the symmetry breaking branch $2\theta = 0$ or π (solid line in figure 7) while for the present solution the phase difference 2θ behaves as an order parameter (gray thick solid line in figure 7) similarly to A_a shown in figure 2(b). We define the last solution as the phase parity breaking branch.

From (13) we find that $\phi_1 + \phi_2 \rightarrow 0$ for $E_{in} \rightarrow 0$, i.e., the cavities tend to oscillate in an antisymmetric way as seen from figure 7(b). If the cavities were linear the even incident wave would excite symmetric oscillations $\phi_1 = \phi_2$ with $\theta = 0$ only provided that $||1 - H_{eff}(\omega)|| \neq 0$. However if the determinant equals zero the antisymmetric cavity's oscillations can be excited independently of the incident wave, i.e., this odd mode is localized and therefore is the BSC whose isolated eigenfrequency is fixed by equation (8). If the frequency of the incident wave coincides with ω_c the odd BSC can be superposed to the even mode [23]. However for the nonlinear case that is not so. First, the BSC frequency becomes dependent on the intensity because of the nonlinear contribution to $\delta\epsilon$ as given by equation (12). Second, the nonlinearity violates the superposition principle. We can rigorously define the BSC for $E_{in} = 0$ only as was obtained above and shown in figures 5 and 7(b) by the bold circles. Indeed, as soon as $E_{in} \neq 0$ the phases of the cavity's oscillations cease to be an antisymmetric mode, and therefore

the BSC begins to couple with the incident wave. In fact, figures 5 and 7(b) show that the symmetry breaking branch and the phase parity breaking branch stem from the BSC point marked by the bold circle. The phenomenon of the BSC in the nonlinear case is discussed in [17, 19].

The transmission amplitude in accordance with equations (10) and (13) becomes

$$t = \frac{J_4 E_{in}}{J_4 + i\Gamma_k}. \quad (16)$$

Therefore the transmission for the phase parity breaking branch has no resonance behavior, as seen from figure 3 by the thick gray solid line.

Because of the phase difference $2\theta \neq 0, \pi$ for the phase parity breaking branch a current can flow between the cavities similar to the tunneling current between two superconducting samples. Multiplying equations (5) by $E_0^* = t^*$ and subtracting the complex conjugated terms one can obtain the value of the power flow current flowing between the chain at the '0'th site and the cavities as follows:

$$j_{0 \rightarrow 1,2} = \epsilon_W J_2 \text{Im}(t\phi_{1,2}^*). \quad (17)$$

Similar manipulations with the cavity's amplitudes give the current between the cavities:

$$j_{1 \rightarrow 2} = J_4 \delta\epsilon \text{Im}(\phi_1 \phi_2^*) = J_4 \delta\epsilon |\sin(2\theta)|. \quad (18)$$

It follows also that the current from the '-1'th site to the '0'th site of the chain coincides with the current from the '0'th site to the '1'th one. Therefore the currents (17) and (18) coincide too in accordance with the Kirchhoff rule. Thus, the input power induces a vortical current between the waveguide and cavities via the coupling J_2 and between the cavities via the coupling J_4 .

6. Power current between cavities

Following the methods developed for a PC waveguide coupled with cavities [17, 19, 24] we calculated the transmission shown in figure 8. Details of the calculation will be given in [25].

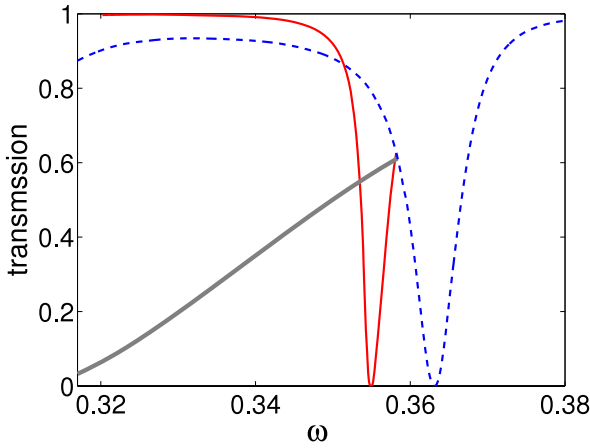


Figure 8. Transmission in the PC structure shown in figure 1(a) for the parameters of the PC: $a = 0.5 \mu\text{m}$, $r_d = 0.18a$, $\epsilon_0 = 11.56$, $\epsilon_d = 3$, $\lambda = 0.05$.

Note the good agreement of the transmission for the PC and the tight-binding model calculations (figure 3). Further, we calculated the electric field directed along the dielectric rods $\mathbf{E}(\mathbf{x})$ and the Poynting vector $\frac{c}{8\pi} \text{Re}(\vec{\mathbf{E}}^* \times \vec{\mathbf{H}}) = \frac{c^2}{8\pi\omega} \text{Im}(\mathbf{E}^* \nabla \mathbf{E})$. The results are collected in three patterns of the current flow in figure 9 corresponding to the three scenarios of the transmission. In the symmetry preserving scenario the current flow on the waveguide is laminar while each cavity

has vortical flows around with opposite directions of flow. In the symmetry breaking scenario one can observe vortical flows around the cavities in the same direction complemented by the current vortex in the waveguide in order to compensate for the vorticity of current flows near the cavities. For the phase parity breaking case the pattern distinctively demonstrates the current flowing between the cavities and the waveguide in full correspondence to the model results.

Thus, our analysis shows that input power can break the symmetry of a system of a linear waveguide coupled with two identical nonlinear off-channel cavities positioned symmetrically relative to the waveguide. The symmetry can be broken because of the different intensities of the EM field at the cavities. Moreover the intensities might be equal but the phases of the oscillations of the EM field in the cavities differ to give rise to the current circulating between the cavities. In general we could assume that the symmetry can be broken both by different intensities and by different phases. However, as then follows from equations (5), we obtained $j_{1 \rightarrow 2} = J_4 \delta \epsilon_2 \sqrt{l_1 l_2} \sin(2\theta)$ while $j_{2 \rightarrow 1} = -J_4 \delta \epsilon_1 \sqrt{l_1 l_2} \sin(2\theta)$, i.e. the Kirchhoff rule would be violated. Therefore this assumption is not valid.

7. Summary

The processes of transmission through a linear waveguide coupled with two nonlinear off-channel resonance cavities

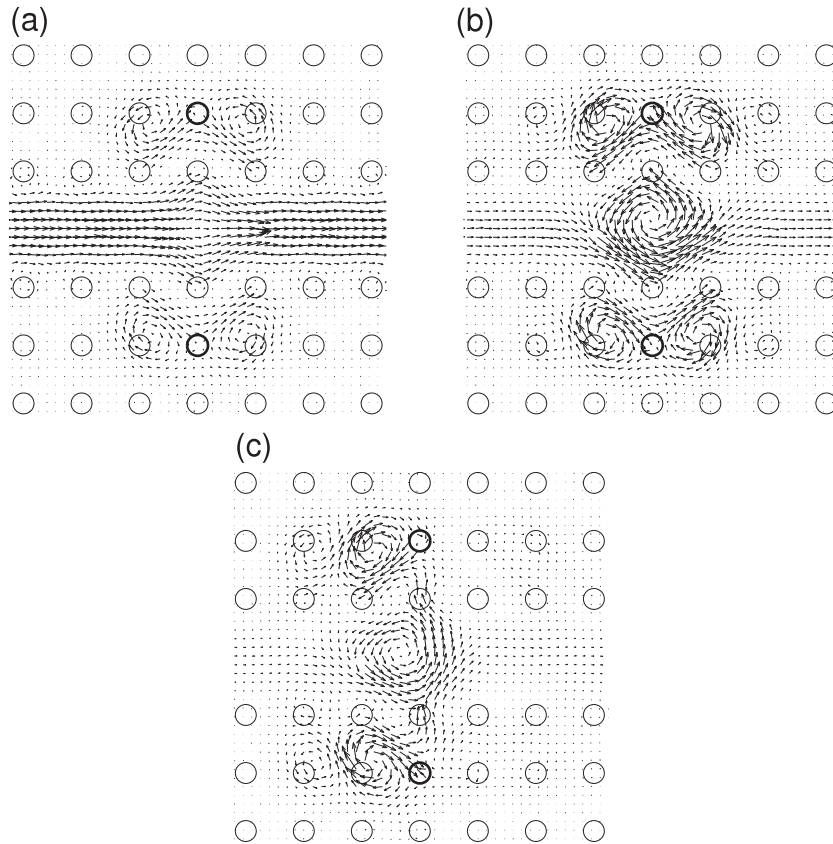


Figure 9. Current flows for the symmetry preserving branch (a), for the symmetry breaking branch (b), and for the phase parity breaking branch (c) for $\frac{\partial \omega}{2\pi c} = 0.34$. The bold circles mark the nonlinear cavities near the waveguide.

coupled with each other display a surprisingly rich variety. For linear defects it is clear that we have a direct process of wave transmission over the waveguide which interferes with the back scattering processes from the off-channel cavities giving rise to zeros of the transmission and the Fano resonances. As was explicitly established in [21], a nonlinearity of the defect leads to nonlinear Fano resonance dependent on frequency and/or incident power. For two nonlinear off-channel defects one can expect two nonlinear Fano resonances as was indeed found in [13–15, 26]. However, our calculations reveal a substantially more sophisticated picture of the transmission. The complexity of the wave transmission in a waveguide coupled with two nonlinear off-channel defects is the result of interference of two back scattering nonlinear processes between each other and with the direct wave transmission in the waveguide.

For the linear case the eigen modes rigorously satisfy the symmetry of permutation of the cavities. As a result we observe only one resonance dip, while the antisymmetric (odd) mode does not participate in the transmission phenomena because of its zero coupling with incident symmetric wave. This mode is obviously the bound state in continuum (BSC) [19, 20]. The oscillations of the EM field at the defects have no phase difference: $2\theta = 0$.

For the nonlinear defects the situation changes crucially. We have three branches. (i) The symmetrical branch with equal amplitudes at the defects $\phi_1 = \phi_2$ inherited from the linear case. There is no phase difference between the EM oscillations at the cavities: $2\theta = 0$. The incident wave supports only the symmetrical mode as shown in figure 2. (ii) The symmetry breaking branch for which the intensities in the cavity defects are not equal: $I_1 > I_2$. There is an equivalent branch with $I_1 < I_2$. These branches break the symmetry relative to the permutation of the cavities. The EM oscillations in the cavities are opposite in phase, $2\theta = \pi$, although they might be in phase at some domain of the incident amplitude as seen from figure 7(b). As shown in figures 2 and 6 the incident wave excites both symmetrical (even) and antisymmetrical (odd) modes. This results in an additional resonance dip in the transmission as shown in figure 3. (iii) The phenomenon of breaking of symmetry by intensities for transmission through a nonlinear system is known [2, 3, 6, 7]. However we reveal one more branch in which the EM oscillations in the nonlinear cavities have the same intensity but different phases. This difference of phases is neither zero nor π but smoothly depends on the frequency and the amplitude of the incident wave as shown in figure 7. If the defects are overlapped the phase difference gives rise to current circulation between the defects. The direction of the current is incidental but its value is given by equations (17) and (18). These model results agree with the

current flow patterns presented in figure 9 in application to a 2D PC with two defect rods spaced symmetrically near the PC waveguide.

Although the nonlinear equations might have steady solutions they must be stable. A stability analysis is performed in [25] which shows that each branch discussed above can exist.

Acknowledgments

The work was supported by RFBR-grant 09-02-98005-‘Siberia’ and by RFBR-grant 11-02-00289.

References

- [1] Landau L D and Lifschitz E M 1980 *Statistical Physics* (Oxford: Pergamon)
- [2] Haelterman M and Mandel P 1990 *Opt. Lett.* **15** 1412
- [3] Longchambon L, Treps N, Coudreau T, Laurat J and Fabre C 2005 *Opt. Lett.* **30** 284
- [4] Fratallocchi A and Assanto G 2006 *Opt. Lett.* **31** 1489
- [5] Dror N and Malomed B A 2009 *Phys. RevE* **79** 016605
- [6] Maes B, Soljačić M, Joannopoulos J D, Bienstman P, Baets R, Gorza S-P and Haelterman M 2006 *Opt. Express* **14** 10678
- [7] Maes B, Bienstman P and Baets R 2008 *Opt. Express* **16** 3069
- [8] Maes B, Fiers M and Bienstman P 2009 *Phys. RevA* **80** 033805
- [9] Otsuka K and Ikeda K 1987 *Opt. Lett.* **12** 599
- [10] Huybrechts K, Morthier G and Maes B 2010 *J. Opt. SocB* **27** 708
- [11] Mingaleev S F, Kivshar Yu S and Sammut R A 2000 *Phys. Rev. E* **62** 5777
- [12] Mingaleev S F and Kivshar Yu S 2001 *Phys. Rev. Lett.* **86** 5474
- [13] Miroshnichenko A E and Kivshar Yu S 2005 *Opt. Express* **13** 3969
- [14] Miroshnichenko A E and Kivshar Yu S 2005 *Phys. RevE* **72** 056611
- [15] McGurn A R 2003 *Chaos* **13** 754
- [16] Busch K, Mingaleev S F, Garcia-Martin A, Schillinger M and Hermann D 2003 *J. Phys.: Condens. Matter* **15** R1233
- [17] Bulgakov E N and Sadreev A F 2010 *Phys. RevB* **81** 115128
- [18] Cowan A R and Young J F 2003 *Phys. RevE* **68** 046606
- [19] Bulgakov E N and Sadreev A F 2009 *Phys. RevB* **80** 115308
- [20] Ladrón de Guevara M L, Claro F and Orellana P A 2003 *Phys. Rev.B* **67** 195335
- [21] Miroshnichenko A E, Mingaleev S F, Flach S and Kivshar Yu S 2005 *Phys. RevE* **71** 036626
- [22] Joannopoulos J, Johnson S G, Winn J N and Meade R D 2008 *Photonic Crystals: Molding the Flow of Light* (Princeton, NJ: Princeton University Press)
- [23] Bulgakov E N, Pichugin K N, Sadreev A F and Rotter I 2006 *JETP Lett.* **84** 508
- [24] Bulgakov E N and Sadreev A F 2008 *Phys. RevB* **78** 075105
- [25] Bulgakov E N, Pichugin K N and Sadreev A F 2011 *Phys. Rev. B* at press
- [26] Miroshnichenko A E 2009 *Phys. RevE* **79** 026611